ACS Photonics

Article

pubs.acs.org/journal/apchd5

Photocurrent Enhancement from Solid-State Triplet−Triplet Annihilation Upconversion of Low-Intensity, Low-Energy Photons

Chuanhao Li,[†,§] Christopher Koenigsmann,[‡,§] Fan Deng,[†] Anna Hagstrom,[†] Charles A. Schmuttenmaer,[*,‡] and Jae-Hong Kim[*,†]

[†]Department of Chemical and Environmental Engineering, Yale University, New Haven, Connecticut 06520-8276, United States

[‡]Yale Energy Sciences Institute and Department of Chemistry, Yale University, New Haven, Connecticut 06520-8107, United States

Supporting Information

ABSTRACT: We present a red-to-blue upconversion system based on triplet−triplet annihilation in a solid-state film configuration that significantly enhances the photocurrent of a model solar cell device. The film is robust against oxygen quenching and can be readily tailored to existing solar cell architectures. The photovoltaic performance of upconversion-assisted dye-sensitized photoelectrochemical cells was measured under both high-power coherent laser and low-power incoherent light irradiation (light-emitting diode and simulated AM1.5G sunlight). By utilizing low-energy photons that would otherwise be wasted, the photocurrent is enhanced by as much as 35% under one-sun light intensity when a model solar cell device is coupled with a TTA film and a reflector.

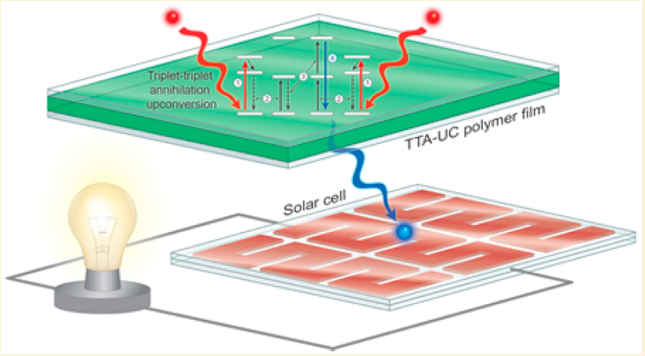

KEYWORDS: *triplet−triplet annihilation, upconversion, solar cells, photoelectrochemical cells*

Effectively harnessing solar energy is widely considered one of the most promising means of more sustainably meeting the growing energy demand. However, solar technologies such as photovoltaics or photocatalytic fuel production cells are inherently limited by the energy range of photons absorbed by their materials. Photons with energy below the band gap in semiconductor-based photovoltaics or below the HOMO−LUMO gap in dye-sensitized photoelectrochemical cells (DSPCs) are not absorbed at all, thereby wasting a large fraction of incoming solar radiation[1] and accounting for the Shockley−Queisser limit in single-junction solar cells.[2,3]

Upconversion (UC) of two or more lower energy photons to a single higher energy photon has the potential to address these challenges.[1,4] Of the two primary UC mechanisms, lanthanide-based UC was the first to be incorporated into solar cells.[5−8] However, this UC approach suffers from very low quantum efficiencies at the low light intensities relevant to solar applications.[6,9] In contrast, organic triplet−triplet annihilation (TTA)-based UC has significantly higher quantum yields of 3−40%, even at realistically low excitation intensities of 1−10 mW·cm^{-2} (one-sun conditions correspond to 100 mW·cm^{-2}).[5,6] Spectral shifting can be tuned via myriad sensitizer and acceptor combinations, which makes TTA-UC useful for a wide variety of solar devices.[10,11] Schmidt et al. achieved the first proof-of-concept TTA-based solar cell device by placing a sealed cuvette with a deoxygenated solution of TTA chromophores in front of an a-Si:H solar cell.[12] Recently, they incorporated a sealed liquid chamber containing a deoxygenated organic TTA solution into a conventional dye-sensitized solar cell.[13] Very recently, more effort has been directed toward utilizing TTA-UC to enhance solar conversion efficiency.[14,15] The reliance of such designs on sealed organic solutions has been dictated by the necessity of a host medium that is sufficiently fluidic to allow facile chromophore diffusion and deoxygenated to prevent oxygen quenching.

Moving forward, research in this field should target solid-state TTA-UC systems that are more conducive to robust integration into in a wide variety of solar device architectures and practical long-term applications. This study reports the first integration of a solid-state TTA-UC polymeric film into a solar cell device. A DSPC was chosen as a model system to demonstrate performance improvement (Figure 1). Photons with energy greater than the HOMO−LUMO gap of the dye are absorbed by the inherent DSPC, while lower energy photons are transmitted to the underlying TTA film. The upconverted photons emitted by the film are reflected back to the active layer of the DSPC and absorbed, thereby leading to an enhancement in the generated photocurrent. A coherent laser, an incoherent light-emitting diode (LED), and the AM1.5G output of a solar simulator are used to demonstrate substantial photocurrent enhancements under a range of illumination conditions.

Received: December 8, 2015
Published: May 2, 2016

DOI: 10.1021/acsphotonics.5b00694
ACS Photonics 2016, 3, 784−790

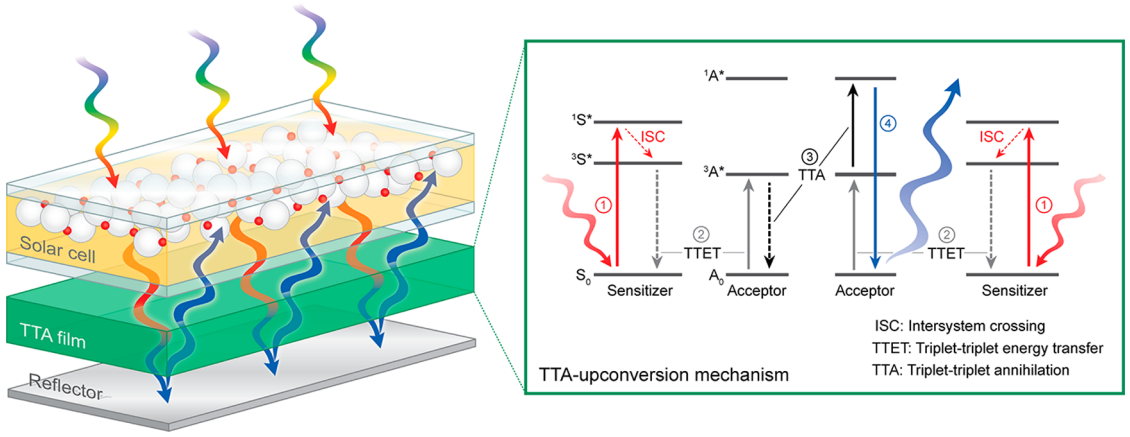

Figure 1. Schematic illustration of TTA film-assisted absorption of photons with energies below the HOMO−LUMO gap of the chromophore sensitizer in a dye-sensitized photoelectrochemical cell.

RESULTS AND DISCUSSION

Polyurethane was chosen as the host matrix for these films due to its ease of manipulation, demonstrated compatibility with TTA-UC, and low oxygen permeability.[16] The film was fabricated between two thin layers of glass, providing mechanical stability and further protection against oxygen permeation. The final thickness of the films was measured to be approximately 3.5 μm using SEM analysis (see Figure S1 in the Supporting Information). Palladium(II) *meso*-tetraphenyltetrabenzoporphyrin (PdTPBP) and perylene were chosen as sensitizer and acceptor, respectively (Figure 2a). PdTPBP has strong absorption peaks centered at 440 nm (Soret band) and 626 nm (Q-band) and emits phosphorescence centered at 792 nm (λ_{ex} = 626 nm). Its strong Q-band absorption (ε = (1.05 ± 0.07) × 10^5 M^{-1} cm^{-1} at 626 nm[17]) ensures efficient capture of red photons. Perylene has an intense $\pi \rightarrow \pi^*$ transition band from 450 to 420 nm, with an associated fluorescence peak centered at 470 nm. Its high fluorescence quantum yield (Φ_f = 0.98) and reasonable thermal and photochemical stability make it an ideal TTA-UC acceptor.[18,19] Selective excitation of PdTPBP at 635 nm in the presence of perylene generates upconverted fluorescence in the blue region centered at 470 nm.

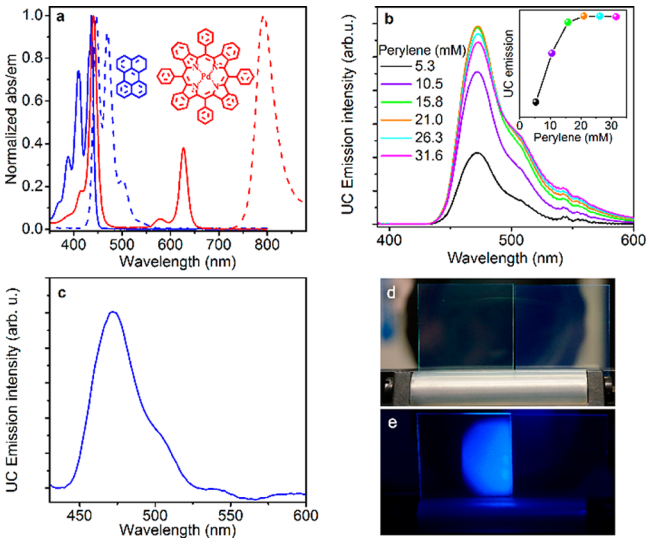

Figure 2. Characterization of TTA-UC films. (a) Normalized absorption (solid lines) and emission (dashed lines) spectra of PdTPBP (red) and perylene (blue) in THF at room temperature. Phosphorescence of PdTPBP was measured after purging the solution with nitrogen gas for 30 min. (b) UC emission spectra of TTA films with different concentrations of perylene. Inset: Integrated UC emission intensity as a function of the perylene concentration. The intensity of laser excitation was 150 mW·cm^{-2}. The concentration of PdTPBP was 1.52 mM. (c) UC emission spectrum of a TTA film upon illumination by a 635 nm laser at 7 mW·cm^{-2}. (d) Photographs of films (left: TTA film, right: control film without PdTPBP). (e) Same as (d), but under 2-sun-equivalent illumination by a solar simulator passed through a 600 nm long-pass filter. UC emission was isolated using a 466 nm bandpass filter.

The perylene concentration was first optimized in order to facilitate efficient triplet−triplet energy transfer (TTET) between PdTPBP and perylene in the polymer matrix and to maximize the resulting UC emission. As shown in Figure 2b, initial increases in perylene concentration at a constant PdTPBP concentration lead to a significant increase in UC emission; that is, excess perylene promotes more effective quenching of PdTPBP. However, increasing the perylene concentration beyond 21 mM provides no additional increase in UC emission, as the quenching by perylene molecules has reached maximum efficiency. Therefore, a perylene concentration of 21 mM was chosen as the optimal concentration for subsequent TTA film fabrication.

UC emission from these films (Figure 2c) was measured under illumination with a 635 nm diode laser at an intensity of 7 mW·cm^{-2},[20] a value approximately equivalent to the integrated intensity of the solar spectrum between 605 and 650 nm (see calculation in Figure S2). The measurable emission peak confirms that these TTA-UC polymer films operate effectively under illumination in low-intensity conditions relevant to solar devices. As shown in Figure 2d and e, bright blue emission is visible to the naked eye under 2-sun-equivalent illumination with simulated sunlight. A control film containing perylene without PdTPBP shows no emission under equivalent illumination, confirming that perylene emission in the TTA-UC films is exclusively a result of the UC process. We found that the efficiency of TTA-UC was virtually unchanged even after 30 days of exposure to ambient conditions (Figure S3). For application to solar devices to be economically feasible, the longevity of TTA-UC systems is a vital concern. While the dyes typically employed for TTA-UC undergo photodegradation when exposed to very high-power illumination, exposure to

DOI: 10.1021/acsphotonics.5b00694
ACS Photonics 2016, 3, 784−790

oxygen actually poses the greatest threat to their longevity and photostability. Quenching of their triplet excited states leads to the formation of singlet oxygen, which in turn leads to chromophore degradation.[1] In solvent-based TTA-UC systems, longevity is contingent on the thoroughness of deoxygenation and quality of the sealing procedures employed (which can be circumvented by using impractical flow-through reactors that cycle the TTA-UC solvent).[21] However, in the TTA-UC films employed herein, the polymer matrix itself affords some protection from diffusion of oxygen into the system,[16] as do the layers of glass. Sealing the edges of the films with epoxy resin makes them even more resistant to oxygen infiltration, thereby extending their operational lifetime significantly. It was previously reported that the photodegradation of dyes is caused by the combined effect of high O_2 concentration and light intensity.[22] A recent report demonstrated that under 1-sun conditions a TTA-UC solution retains its initial performance for up to 1000 h.[1] Thus, it is reasonable to expect that our TTA-UC films, which we demonstrate to be O_2-resistant, would exhibit excellent photostability under illumination by sunlight.

Having confirmed efficient and robust film function under ambient conditions, we turned our focus to integration of the films into a model solar cell architecture. We employed the I^-/I_3^- redox couple, a platinized fluorine doped tin oxide (FTO) cathode, and a dye-sensitized mesoporous TiO_2-coated FTO glass photoanode and placed a TTA film behind this DSPC cell. The dye selected was D131 (2-cyano-3-[4-[4-(2,2-diphenylethenyl)phenyl]-1,2,3,3a,4,8b-hexahydrocyclopent[*b*]-indol-7-yl]-2-propenoic acid, Figure S4) because it provides an ideal spectral match for the red-to-blue TTA-UC system; that is, it absorbs the UC emission from perylene but not the red light used to excite PdTPBP. DSPCs with different sensitizing dyes could easily employ different TTA-UC chromophore pairs that provide different spectral shifting schemes. D131 is particularly appealing since it is an indoline dye, one of the types of metal-free organic dyes that have shown efficiencies comparable to the ruthenium-based dyes commonly applied in DSPCs.[23,24] Such organic dyes have been the subject of recent interest for their high extinction coefficients without a need for costly precious metals.[25,26]

As shown in Figure S3, the D131 molecule has a typical donor–π bridge–acceptor structure in which the indoline unit acts as the donor moiety, while cyanoacrylate acts as both the acceptor and the anchoring group to the surface of TiO_2.[27−29] Its absorption onset wavelength is 530 nm, which corresponds to a HOMO–LUMO gap of ∼2.34 eV. Under operating conditions in a DSPC, the external quantum efficiency (EQE) spectrum, referring to the number of incident photons at a given wavelength that successfully produce charged carriers, broadens and the absorption onset is considerably red-shifted to 575 nm (Figure 3a). The EQE in the range of wavelengths emitted by the TTA-UC films is between 75% and 80% of its maximum, which could potentially provide a substantial enhancement in device efficiency.

The photovoltaic performance of the D131-sensitized TiO_2 cells is summarized in Table S1 and Figure S5. TiO_2 layer thicknesses of 5 and 10 μm were found to be optimal for demonstrating performance enhancement from TTA film incorporation, as discussed below. To verify the quality of our devices, we constructed a DPSC with a 25 μm TiO_2 layer, which yielded an efficiency of 5%, which is consistent with or better than prior reports.[27−29] Interestingly, the thinner films

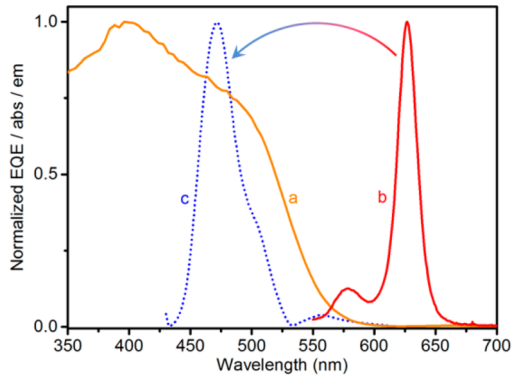

Figure 3. Normalized (a) external quantum efficiency (EQE) spectrum of a D131-sensitized TiO_2 photoelectrochemical cell, (b) Q-band absorption of PdTPBP, and (c) UC upconversion emission spectrum of a TTA-UC film.

optimized for demonstrating the TTA-UC enhancement yielded only slightly lower efficiencies of 4.3% and 4.7% for the 5 and 10 μm thick layers, respectively.

The UC power dependence was determined by measuring UC emission intensity as a function of excitation intensity. Because the intensity of TTA-UC depends on the concentration of chromophores in triplet excited states, it is also inherently dependent on excitation intensity.[6] Results are shown on a log–log plot in Figure 4a (triangle), and the

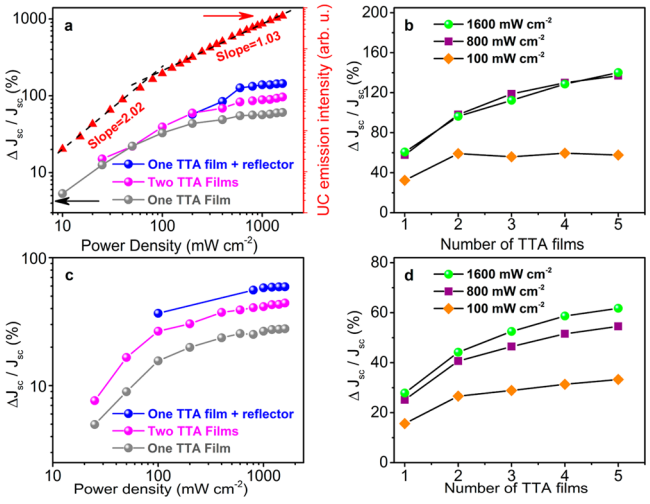

Figure 4. TTA-UC J_{sc} enhancement under 635 nm laser illumination. (a) Intensity of UC emission from the films (triangle) and TTA-UC J_{sc} enhancement (circle) as a function of incident intensity in DSPCs with a 5 μm thick TiO_2 layer. (b) J_{sc} enhancement as a function of the number of TTA films under illumination at various intensities in DSPCs with a 5 μm thick TiO_2 layer. (c) Same as (a), but with a 10 μm thick TiO_2 layer. (d) Same as (b), but with a 10 μm thick TiO_2 layer.

corresponding emission spectra are shown in Figure S6. At excitation intensities below 100 mW·cm^{-2}, a linear fit of the log–log plot has a slope of 2.02, indicating a quadratic dependence on the intensity. On the other hand, at incident intensities above 100 mW·cm^{-2}, a linear fit of the log–log plot has a slope of 1.03, indicating a linear intensity dependence. These values are consistent with the established kinetics of the TTA-UC process. That is, under low power excitation, depopulation of the acceptor's triplet states is dominated by

DOI: 10.1021/acsphotonics.5b00694
ACS Photonics 2016, 3, 784−790

pseudo-first-order decay, and UC emission intensity has a quadratic dependence on excitation power as expected for a bimolecular process. However, under excitation at a sufficiently high power, TTA overtakes pseudo-first-order decay as the dominant ^{3}A* depopulation process, and TTA-UC intensity becomes linearly dependent on excitation power.[30−32] In our films, this crossover to maximum efficiency TTA occurs at a relatively low intensity of ∼80 mW·cm^{-2}.

The dependence of DSPC performance on excitation intensity when integrated with TTA-UC films was also characterized. The DSPC enhancement provided by TTA-film incorporation was defined as the percent difference between the short-circuit current density (J_{sc}) of the DSPC with and without the film at a given illumination intensity ($\Delta J_{sc}/J_{sc} \times 100\%$). In the case of experiments with a reflector, the performance of the device was benchmarked with the reflector in place so that the enhancement in performance was attributed solely to the addition of the TTA film. Given the established dependence of DSPC performance on TiO_2 layer thickness,[33] we measured the intensity-dependent enhancement in DSPCs with mesoporous TiO_2 layers of both 5 μm (Figure 4a: circle) and 10 μm (Figure 4c) thickness. J_{sc} enhancements of well over 100% were achieved for the DSPCs with 5 μm layers of TiO_2 and a reflector (Figure 4a). The trends in J_{sc} enhancement for both sets of DSPCs (Figure 4a: circle, Figure 4c) are similar to those of the TTA-UC emission intensity (Figure 4a: triangle), showing a transition from a higher to a lower intensity dependence at ∼100 mW·cm^{-2}. This finding illustrates that, as one would expect, the enhancement in DSPC photocurrent is closely related to the intensity of UC emission from the TTA film. Even under very low intensity excitation at 10 mW·cm^{-2}, the photocurrent was enhanced by 5.3%. In addition to examining the enhancement in photocurrent, we also observed a small enhancement in the open-circuit voltage (V_{oc}) induced by the TTA-UC films, and the results are summarized in Figure S7. The enhancement is slightly higher for lower excitation intensities.

To better harvest TTA-UC emission for photocurrent enhancement, we placed a reflector behind the film to redirect UC fluorescence back toward the active layer of the solar cell and thereby increase the fraction of UC fluorescence absorbed by the device.[34] In order to selectively reflect back the upconverted blue emission, we used a 567 nm long-pass filter that reflects blue wavelengths but transmits the red excitation light. Incorporation of this reflector led to an impressive 2-fold increase in photocurrent at excitation intensities above 400 mW·cm^{-2} (Figure 4a,c: blue circle), while no changes were observed in the control experiments with the reflector but without TTA films. Adding a second TTA film to the DSPC in order to harvest a greater fraction of the red excitation radiation also increased the photocurrent relative to the initial single-film setup (Figure 4a,c: magenta circle), as expected, though significantly less so than the reflector. The smaller magnitude of this increase was not surprising since PdTPBP has a very high molar extinction coefficient for red excitation (ε = 1.05 × 10^5 M^{-1}·cm^{-1} at 626 nm, Figure 2a), and the first TTA film absorbs nearly all of the incident photons.

In addition, we measured the enhancement in photocurrent with up to five TTA-UC films under three different excitation intensities (Figure 4b,d). Under higher intensity illumination (800, 1600 mW·cm^{-2}), the photocurrent increases with addition of each successive TTA film, as more incident radiation is captured and upconverted. Under lower intensity illumination (100 mW·cm^{-2}), on the other hand, increasing the number of TTA films above two provided no significant enhancement, especially with the 5 μm TiO_2 layer, indicating that two films are sufficient to capture most incident radiation at this intensity. It is reasonable to expect that at the lower intensities of solar radiation (i.e., on the order of 7 mW·cm^{-2} in the Q-band absorption region of PdTPBP, *vide supra*) a single TTA film will be sufficient.

Although overall trends were similar, the DSPCs with 10 μm TiO_2 layers showed consistently lower photocurrent enhancement over the range of incident intensity than those with 5 μm TiO_2 layers (note the difference in vertical axis scales in Figures 4a and 4c). This is because thicker layers of TiO_2 absorb and scatter a higher fraction of the incident radiation, and therefore a smaller fraction reaches the TTA-UC film to contribute to photocurrent enhancement. Upon increasing excitation intensity from 800 to 1600 mW·cm^{-2}, negligible additional enhancement was observed with 5 μm TiO_2 layers due to saturation of TTA-UC in the film as discussed above (Figure 4b). On the other hand, when using 10 μm TiO_2 layers (albeit detrimental to transmittance of excitation illumination), the TTA-UC films are not similarly saturated at 800 mW·cm^{-2}, as increasing the excitation intensity to 1600 mW·cm^{-2} provides an additional increase in photocurrent (Figure 4d).

One of the primary advantages of TTA-UC over lanthanide-based UC, which requires high-intensity coherent radiation from lasers, is its ability to operate efficiently using incoherent radiation such as sunlight.[35] A large body of research currently focuses on developing TTA-UC systems that operate efficiently with low-intensity, incoherent excitation sources, which is crucial for practical enhancement of solar applications through TTA-UC. As part of this effort, LEDs have been widely employed to demonstrate TTA-UC under these conditions.[36,37] LEDs emit radiation that is incoherent but still relatively monochromatic, retaining the useful ability of lasers to selectively probe responses to particular wavelength ranges. For our initial investigation of the performance of our TTA-UC films under low-intensity incoherent illumination, we employed a red LED (625 nm, full width at half-maximum of 16 nm) with its power adjusted to approximate the intensity of red photons present in under one- and two-sun illumination (7 and 14 mW·cm^{-2}, respectively).

The resulting photovoltaic performance is summarized in Figure 5. In DSPCs with 5 μm thick mesoporous TiO_2 layers and a single TTA film (Figure 5a), the photocurrent was enhanced by 13.6% and 20.3% upon illumination with the equivalent of one-sun and two-suns, respectively. Adding a rear reflector to more effectively utilize the emitted blue photons

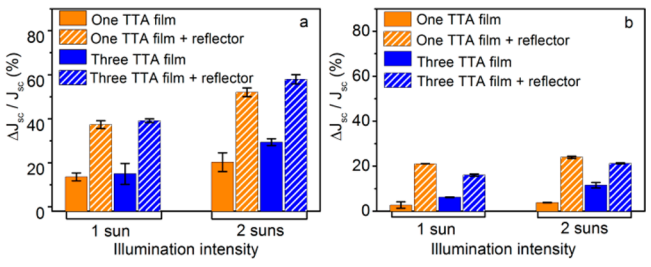

Figure 5. TTA-UC-induced J_{sc} enhancement using LED (wavelength centered at 625 nm) illumination of DSPC devices with (a) 5 μm and (b) 10 μm sensitized TiO_2 layer thicknesses. Error bars represent standard deviation of 5 measurements.

DOI: 10.1021/acsphotonics.5b00694
ACS Photonics 2016, 3, 784−790

increases these enhancements to 37.3% and 52.0%, relative to the device with the rear reflector only. As expected from the trends observed with coherent laser illumination, photocurrent enhancements are only slightly higher when the number of TTA films in the DSPCs is increased from one to three. This implies that a single TTA film is already capable of absorbing most of the excitation photons at these relatively low illumination intensities. When the thickness of the mesoporous TiO_2 layers is increased from 5 μm (Figure 5a) to 10 μm (Figure 5b), the overall trends in J_{sc} remain the same, but the resulting enhancement values are significantly lower, since the thicker layer of TiO_2 interferes with effective transmission of red photons to the TTA films as previously discussed. Overall, the greatest enhancement of 57.9% was provided by the device consisting of a 5-μm mesoporous TiO_2 layer coupled with three TTA films and a reflector under two-sun illumination.

Finally, in order to most realistically approximate the performance of the TTA-enhanced DSPCs under solar radiation, we used a solar simulator equipped with a 300 W ozone-free xenon lamp and an AM1.5G filter as excitation source. Under one- and two-sun equivalents of illumination, the blue UC fluorescence of the TTA film-enhanced DSPCs was readily visible to the naked eye (see Figure 2e and video in the SI). Under one-sun excitation, DSPCs with 5 μm layers of TiO_2 and a single TTA film showed a 4.2% enhancement in photocurrent, which increased to 18.8% upon incorporation of a rear reflector (Figure 6a). Under two-sun illumination, the

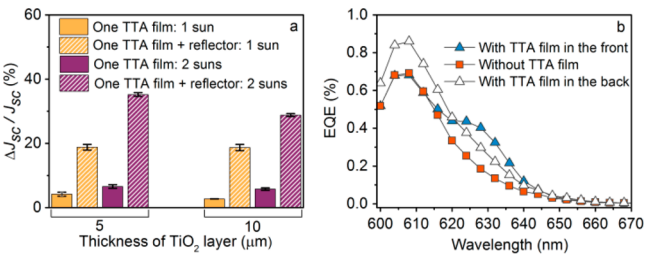

Figure 6. (a) TTA-UC-induced J_{sc} enhancement using simulated AM1.5G light as the light source. (b) EQE spectra of solar cells with and without integrated TTA films under two-sun illumination. A 600 nm long-pass filter was used to isolate the red region of the solar spectrum.

same DSPCs showed corresponding photocurrent enhancements of 6.6% and 35.2%, respectively. Similar trends in photocurrent enhancement were found when using DSPC devices with 10 μm layers of TiO_2 and a single TTA film.

EQE spectra were collected to characterize DSPC enhancement as a function of excitation wavelength (Figure 6b). Incorporation of a TTA film behind the active layer of the DSPC, which is the configuration employed in all above experiments, leads to a significant enhancement in EQE from 600 to 650 nm. Placing the TTA film in the front of the DSPC instead of behind gives rise to EQE enhancement that is greater from 620 to 640 nm but insignificant at shorter wavelengths (Figure 6b). In this configuration, the TTA film is exposed to the full intensity of incident radiation without any obstruction from the DSPC semiconductor layer, blue emission is maximized, and peak EQE enhancement occurs near the absorption maximum of PdTPBP. However, under full-spectrum illumination, parasitic absorption of incident blue photons by the TTA film decreases the number of photons that reach the active layer of the DSPC, ultimately giving rise to lower photocurrents. Partial absorption of incident photons at 600−620 nm by the DSPC active layer also decreases the EQE. These results collectively indicate that the TTA film is most effective when placed behind the DSPC and combined with a rear reflector, where it allows the active layer to be exposed to the full intensity of incident illumination.

CONCLUSION

This study is the first to combine TTA-UC enhancement of solar device performance with the ability to embed the chromophores in polymer matrices that can be easily tailored to films of many different shapes and sizes (Figure S8). The synthetic flexibility and longevity of these TTA-UC films are an important step toward logistically and economically practical applications in solar devices. We demonstrate for the first time that the photocurrent can be enhanced by as much as 35% under illumination by AM1.5G light when a DSPC device is coupled with a TTA film and a reflector. EQE spectra clearly show that TTA-UC makes it possible to generate photocurrent using low-energy photons. Although we used DSPCs as a model device to demonstrate the great promise of TTA-UC for enhancements in efficiency, TTA-UC films are equally compatible with other solar device architectures via rational selection of appropriate sensitizer and acceptor chromophores. For example, our ongoing research focuses on optimizing the TTA-UC chromophore pairs to provide spectral shifting schemes that are compatible with high-performance sensitizers for DSPCs. A large body of research currently focuses on extending the absorption and emission ranges of TTA chromophores,[38,39] and thus we expect to realize even larger enhancements in a broader range of solar devices in the future as this field advances.

METHODS

Preparation and characterization of TTA films and fabrication of DSPC cells are shown in section 1 in the Supporting Information. TTA films were attached behind the DSPCs. DSPC performance was characterized by current density−voltage (J−V) curves measured using a Keithley 2400-C source-meter. For the studies involving the laser excitation source, a 635 nm incident laser (Opto Engine LLC, MRL-III-635-300 mW) was used as the coherent light source equipped with an iris to adjust the beam size. Power was monitored by a Nova II power meter connected with a sensor (OPHIR, PD300 P/N 7Z02410). For the studies involving the LED source, a high-power LED (Thorlabs, M625L3, 625 nm) was used as noncoherent light source. The light passed through an iris, and the excitation intensity was adjusted to 7 mW·cm^{-2} (one-sun) and 14 mW·cm^{-2} (two-suns), respectively. For the studies using simulated solar light, a solar simulator (Newport) equipped with a 300 W ozone-free xenon lamp and AM1.5G filter was used as light source. A focusing lens was placed in the front of the solar cell device to increase the intensity to two suns. The light intensity was adjusted with a diode calibrated by Newport to ASTM E948-09 and E1021-06 standards. For TTA-enhanced photovoltaic tests, a long-pass filter (Thorlabs, FEL 0600-1 V) was used to block the short-wavelength photons. A long-pass dichroic mirror (Thorlabs, DMLP567, 567 nm) was used as the reflector. For the external quantum efficiency measurement, the light was concentrated by a factor of 2.

The J_{sc} enhancement was calculated with

DOI: 10.1021/acsphotonics.5b00694
ACS Photonics 2016, 3, 784−790

$$\Delta J_{sc}/J_{sc} = \frac{J_{sc}(\text{with TTA film}) - J_{sc}(\text{without TTA film})}{J_{sc}(\text{without TTA film})} \times 100\%$$

■ ASSOCIATED CONTENT

Supporting Information

The Supporting Information is available free of charge on the ACS Publications website at DOI: 10.1021/acsphotonics.5b00694.

Additional details regarding experimental methods, SEM images, durability of TTA film, absorption spectrum of D131 dye, photovoltaic performance of D131-sensizited TiO_2, power-dependent TTA-UC emission spectra, TTA-UC-induced V_{oc} change, TTA-UC films with different shapes (PDF)

Video showing the TTA-UC emission under one-sun-equivalent illumination (AVI)

■ AUTHOR INFORMATION

Corresponding Authors

*E-mail: charles.schmuttenmaer@yale.edu.

*E-mail: jaehong.kim@yale.edu.

Author Contributions

§C. Li and C. Koenigsmann contributed equally.

Notes

The authors declare no competing financial interest.

■ ACKNOWLEDGMENTS

This work was funded by the National Science Foundation under grant CBET #1335934 and a generous donation from the TomKat Charitable Trust.

■ REFERENCES

(1) Schulze, T. F.; Schmidt, T. W. Photochemical upconversion: present status and prospects for its application to solar energy conversion. *Energy Environ. Sci.* **2015**, *8*, 103−125.

(2) Shockley, W.; Queisser, H. J. Detailed Balance Limit of Efficiency of p-n Junction Solar Cells. *J. Appl. Phys.* **1961**, *32*, 510−519.

(3) Hagfeldt, A.; Boschloo, G.; Sun, L.; Kloo, L.; Pettersson, H. Dye-Sensitized Solar Cells. *Chem. Rev.* **2010**, *110*, 6595−6663.

(4) Trupke, T.; Green, M. A.; Würfel, P. Improving solar cell efficiencies by up-conversion of sub-band-gap light. *J. Appl. Phys.* **2002**, *92*, 4117−4122.

(5) van Sark, W.; de Wild, J.; Rath, J.; Meijerink, A.; Schropp, R. Upconversion in solar cells. *Nanoscale Res. Lett.* **2013**, *8*, 1−10.

(6) Zhou, J.; Liu, Q.; Feng, W.; Sun, Y.; Li, F. Upconversion Luminescent Materials: Advances and Applications. *Chem. Rev.* **2015**, *115*, 395−465.

(7) de Wild, J.; Meijerink, A.; Rath, J. K.; van Sark, W. G. J. H. M.; Schropp, R. E. I. Upconverter solar cells: materials and applications. *Energy Environ. Sci.* **2011**, *4*, 4835−4848.

(8) Ramasamy, P.; Manivasakan, P.; Kim, J. Upconversion nanophosphors for solar cell applications. *RSC Adv.* **2014**, *4*, 34873−34895.

(9) Cates, E. L.; Chinnapongse, S. L.; Kim, J.-H.; Kim, J.-H. Engineering Light: Advances in Wavelength Conversion Materials for Energy and Environmental Technologies. *Environ. Sci. Technol.* **2012**, *46*, 12316−12328.

(10) Singh-Rachford, T. N.; Castellano, F. N. Photon upconversion based on sensitized triplet−triplet annihilation. *Coord. Chem. Rev.* **2010**, *254*, 2560−2573.

(11) Zhao, J.; Ji, S.; Guo, H. Triplet-triplet annihilation based upconversion: from triplet sensitizers and triplet acceptors to upconversion quantum yields. *RSC Adv.* **2011**, *1*, 937−950.

(12) Cheng, Y. Y.; Fuckel, B.; MacQueen, R. W.; Khoury, T.; Clady, R. G. C. R.; Schulze, T. F.; Ekins-Daukes, N. J.; Crossley, M. J.; Stannowski, B.; Lips, K.; Schmidt, T. W. Improving the light-harvesting of amorphous silicon solar cells with photochemical upconversion. *Energy Environ. Sci.* **2012**, *5*, 6953−6959.

(13) Nattestad, A.; Cheng, Y. Y.; MacQueen, R. W.; Schulze, T. F.; Thompson, F. W.; Mozer, A. J.; Fückel, B.; Khoury, T.; Crossley, M. J.; Lips, K.; Wallace, G. G.; Schmidt, T. W. Dye-Sensitized Solar Cell with Integrated Triplet−Triplet Annihilation Upconversion System. *J. Phys. Chem. Lett.* **2013**, *4*, 2073−2078.

(14) Monguzzi, A.; Borisov, S. M.; Pedrini, J.; Klimant, I.; Salvalaggio, M.; Biagini, P.; Melchiorre, F.; Lelii, C.; Meinardi, F. Efficient Broadband Triplet−Triplet Annihilation-Assisted Photon Upconversion at Subsolar Irradiance in Fully Organic Systems. *Adv. Funct. Mater.* **2015**, *25*, 5617−5624.

(15) Cheng, Y. Y.; Nattestad, A.; Schulze, T. F.; MacQueen, R. W.; Fuckel, B.; Lips, K.; Wallace, G. G.; Khoury, T.; Crossley, M. J.; Schmidt, T. W. Increased upconversion performance for thin film solar cells: a trimolecular composition. *Chem. Sci.* **2016**, *7*, 559−568.

(16) Kim, J.-H.; Deng, F.; Castellano, F. N.; Kim, J.-H. High Efficiency Low-Power Upconverting Soft Materials. *Chem. Mater.* **2012**, *24*, 2250−2252.

(17) Rogers, J. E.; Nguyen, K. A.; Hufnagle, D. C.; McLean, D. G.; Su, W.; Gossett, K. M.; Burke, A. R.; Vinogradov, S. A.; Pachter, R.; Fleitz, P. A. Observation and Interpretation of Annulated Porphyrins: Studies on the Photophysical Properties of meso-Tetraphenylmetalloporphyrins. *J. Phys. Chem. A* **2003**, *107*, 11331−11339.

(18) Cui, X.; Charaf-Eddin, A.; Wang, J.; Le Guennic, B.; Zhao, J.; Jacquemin, D. Perylene-Derived Triplet Acceptors with Optimized Excited State Energy Levels for Triplet−Triplet Annihilation Assisted Upconversion. *J. Org. Chem.* **2014**, *79*, 2038−2048.

(19) Sugunan, S. K.; Tripathy, U.; Brunet, S. M. K.; Paige, M. F.; Steer, R. P. Mechanisms of Low-Power Noncoherent Photon Upconversion in Metalloporphyrin−Organic Blue Emitter Systems in Solution. *J. Phys. Chem. A* **2009**, *113*, 8548−8556.

(20) Standard solar constant and zero air mass solar spectral irradiance tables. American Society for Testing Materials Standard E490-00a, 2014.

(21) Borjesson, K.; Dzebo, D.; Albinsson, B.; Moth-Poulsen, K. Photon upconversion facilitated molecular solar energy storage. *J. Mater. Chem. A* **2013**, *1*, 8521−8524.

(22) Borisov, S. M.; Larndorfer, C.; Klimant, I. Triplet−Triplet Annihilation-Based Anti-Stokes Oxygen Sensing Materials with a Very Broad Dynamic Range. *Adv. Funct. Mater.* **2012**, *22*, 4360−4368.

(23) El-Zohry, A. M.; Roca-Sanjuán, D.; Zietz, B. Ultrafast Twisting of the Indoline Donor Unit Utilized in Solar Cell Dyes: Experimental and Theoretical Studies. *J. Phys. Chem. C* **2015**, *119*, 2249−2259.

(24) Ito, S.; Miura, H.; Uchida, S.; Takata, M.; Sumioka, K.; Liska, P.; Comte, P.; Pechy, P.; Gratzel, M. High-conversion-efficiency organic dye-sensitized solar cells with a novel indoline dye. *Chem. Commun.* **2008**, 5194−5196.

(25) Liang, M.; Chen, J. Arylamine organic dyes for dye-sensitized solar cells. *Chem. Soc. Rev.* **2013**, *42*, 3453−3488.

(26) Mishra, A.; Fischer, M. K. R.; Bäuerle, P. Metal-Free Organic Dyes for Dye-Sensitized Solar Cells: From Structure: Property Relationships to Design Rules. *Angew. Chem., Int. Ed.* **2009**, *48*, 2474−2499.

(27) Hosni, M.; Kusumawati, Y.; Farhat, S.; Jouini, N.; Ivansyah, A. L.; Martoprawiro, M. A.; Pauporté, T. Ruthenium Polypyridyl TG6 Dye for the Sensitization of Nanoparticle and Nanocrystallite Spherical Aggregate Photoelectrodes. *ACS Appl. Mater. Interfaces* **2015**, *7*, 1568−1577.

(28) Rudolph, M.; Yoshida, T.; Miura, H.; Schlettwein, D. Improvement of Light Harvesting by Addition of a Long-Wavelength Absorber in Dye-Sensitized Solar Cells Based on ZnO and Indoline Dyes. *J. Phys. Chem. C* **2015**, *119*, 1298−1311.

(29) Wang, Z.; Wang, X.-F.; Yokoyama, D.; Sasabe, H.; Kido, J.; Liu, Z.; Tian, W.; Kitao, O.; Ikeuchi, T.; Sasaki, S. -i. Esterification of

DOI: 10.1021/acsphotonics.5b00694
ACS Photonics 2016, 3, 784−790

Indoline-Based Small-Molecule Donors for Efficient Co-evaporated Organic Photovoltaics. *J. Phys. Chem. C* **2014**, *118*, 14785−14794.
(30) Haefele, A.; Blumhoff, J.; Khnayzer, R. S.; Castellano, F. N. Getting to the (Square) Root of the Problem: How to Make Noncoherent Pumped Upconversion Linear. *J. Phys. Chem. Lett.* **2012**, *3*, 299−303.
(31) Cheng, Y. Y.; Khoury, T.; Clady, R. G. C. R.; Tayebjee, M. J. Y.; Ekins-Daukes, N. J.; Crossley, M. J.; Schmidt, T. W. On the efficiency limit of triplet-triplet annihilation for photochemical upconversion. *Phys. Chem. Chem. Phys.* **2010**, *12*, 66−71.
(32) Schmidt, T. W.; Castellano, F. N. Photochemical Upconversion: The Primacy of Kinetics. *J. Phys. Chem. Lett.* **2014**, *5*, 4062−4072.
(33) Ito, S.; Zakeeruddin, S. M.; Humphry-Baker, R.; Liska, P.; Charvet, R.; Comte, P.; Nazeeruddin, M. K.; Péchy, P.; Takata, M.; Miura, H.; Uchida, S.; Grätzel, M. High-Efficiency Organic-Dye-Sensitized Solar Cells Controlled by Nanocrystalline-TiO2 Electrode Thickness. *Adv. Mater.* **2006**, *18*, 1202−1205.
(34) Schulze, T. F.; Cheng, Y. Y.; Fückel, B.; MacQueen, R. W.; Danos, A.; Davis, N. J. L. K.; Tayebjee, M. J. Y.; Khoury, T.; Clady, R. G. C. R.; Ekins-Daukes, N. J.; Crossley, M. J.; Stannowski, B.; Lips, K.; Schmidt, T. W. Photochemical Upconversion Enhanced Solar Cells: Effect of a Back Reflector. *Aust. J. Chem.* **2012**, *65*, 480−485.
(35) Baluschev, S.; Miteva, T.; Yakutkin, V.; Nelles, G.; Yasuda, A.; Wegner, G. Up-Conversion Fluorescence: Noncoherent Excitation by Sunlight. *Phys. Rev. Lett.* **2006**, *97*, 143903.
(36) Deng, F.; Francis, A. J.; Weare, W. W.; Castellano, F. N. Photochemical upconversion and triplet annihilation limit from a boron dipyrromethene emitter. *Photochem. Photobiol. Sci.* **2015**, *14*, 1265−1270.
(37) Wang, W.; Liu, Q.; Zhan, C.; Barhoumi, A.; Yang, T.; Wylie, R. G.; Armstrong, P. A.; Kohane, D. S. Efficient Triplet−Triplet Annihilation-Based Upconversion for Nanoparticle Phototargeting. *Nano Lett.* **2015**, *15*, 6332−6338.
(38) Deng, F.; Sun, W.; Castellano, F. N. Texaphyrin sensitized near-IR-to-visible photon upconversion. *Photochem. Photobiol. Sci.* **2014**, *13*, 813−819.
(39) Olivier, J.-H.; Bai, Y.; Uh, H.; Yoo, H.; Therien, M. J.; Castellano, F. N. Near-Infrared-to-Visible Photon Upconversion Enabled by Conjugated Porphyrinic Sensitizers under Low-Power Noncoherent Illumination. *J. Phys. Chem. A* **2015**, *119*, 5642−5649.

DOI: 10.1021/acsphotonics.5b00694
ACS Photonics 2016, 3, 784−790